Protein Science (1999), *8*:873–882. Cambridge University Press. Printed in the USA.

The compact and expanded denatured conformations of apomyoglobin in the methanol–water solvent

YUJI O. KAMATARI,[1,2] SHOKO OHJI,[1] TAKASHI KONNO,[3] YASUTAKA SEKI,[4] KUNITSUGU SODA,[4] MIKIO KATAOKA,[5] AND KAZUYUKI AKASAKA[1,6]

[1]The Graduate School of Science and Technology, Kobe University, Kobe 657-8501, Japan
[2]Oxford Centre for Molecular Sciences, University of Oxford, Oxford OX1 3QT, United Kingdom
[3]National Institute for Physiological Science, Myodaiji, Okazaki 444-8585, Japan
[4]Department of Bioengineering, Faculty of Engineering, Nagaoka University of Technology, Nagaoka 940-2188, Japan
[5]Graduate School of Materials Science, Nara Institute of Science and Technology, Ikoma 630-0101, Japan
[6]Department of Chemistry, Faculty of Science, Kobe University, Kobe 657-8501, Japan

(RECEIVED August 31, 1998; ACCEPTED December 16, 1998)

Abstract

We have performed a detailed study of methanol-induced conformational transitions of horse heart apomyoglobin (apoMb) to investigate the existence of the compact and expanded denatured states. A combination of far- and near-ultraviolet circular dichroism, NMR spectroscopy, and small-angle X-ray scattering (SAXS) was used, allowing a phase diagram to be constructed as a function of pH and the methanol concentration. The phase diagram contains four conformational states, the native (N), acid-denatured (U_A), compact denatured (I_M), and expanded helical denatured (H) states, and indicates that the compact denatured state (I_M) is stable under relatively mild denaturing conditions, whereas the expanded denatured states (U_A and H) are realized under extreme conditions of pH (strong electric repulsion) or alcohol concentration (weak hydrophobic interaction). The results of this study, together with many previous studies in the literature, indicate the general existence of the compact denatured states not only in the salt-pH plane but also in the alcohol-pH plane. Furthermore, to determine the general feature of the H conformation we used several proteins including ubiquitin, ribonuclease A, α-lactalbumin, β-lactoglobulin, and *Streptomyces* subtilisin inhibitor (SSI) in addition to apoMb. SAXS studies of these proteins in 60% methanol showed that the H states of these all proteins have expanded and nonglobular conformations. The qualitative agreement of the experimental data with computer-simulated Kratky profiles also supports this structural feature of the H state.

Keywords: apomyoglobin; expanded helical denatured state; methanol-induced conformational transition; molten globule state; small-angle X-ray scattering

It is increasingly recognized that the structure of non-native states of proteins can provide significant insight into fundamental issues such as the relationship between the sequence of a protein and its three-dimensional structure, the nature of protein-folding pathways, the stability of proteins and their turnover in the cell, and the transport of proteins across membranes. In contrast to the large amount of structural information about native folded proteins, however, only a limited number of denatured proteins have been examined in detail. It is therefore of considerable value to study a wide range of non-native states. One of the most well-studied cosolvents that modifies protein structure is alcohol. Furthermore, the alcohol-induced conformational transitions are also interesting because of the similarity between these conditions and these near the membrane surface (Bychkova et al., 1996). For example, some alcohol-induced molten globule states have been observed at moderately low pH and moderately low dielectric constant (Bychkova et al., 1996; Kamatari et al., 1996; Uversky et al., 1997). These conditions could be similar to those existing near negatively charged membrane surfaces (Bychkova et al., 1996; Uversky et al., 1997). Therefore, these studies may give insight into the mechanism of denaturation of proteins in living cell. Previously, we studied the detail of the methanol-induced conformational transition of cytochrome *c* (Kamatari et al., 1996) and lysozyme (Kamatari et al., 1998) and found a large difference between them. A compact denatured conformation is accumulated during the transition of cytochrome *c*, but the transition of lysozyme is quite cooperative.

Reprint requests to: Kazuyuki Akasaka, The Graduate School of Science and Technology, Kobe University, 1-1 Rokko-dai, Nada-ku, Kobe 657-8501, Japan; e-mail: akasaka@kobe-u.ac.jp.

Abbreviations: apoMb, apomyoglobin; CD, circular dichroism; GdnHCl, guanidine hydrochloride; *H*, expanded helical denatured state; I_M, compact denatured state in methanol; MG, molten globule state; *N*, native state; NMR, nuclear magnetic resonance; ppm, parts per million; R_g, radius of gyration; SAXS, small-angle X-ray scattering; SSI, *Streptomyces* subtilisin inhibitor; TCA, trichloroacetate; TFE, 2,2,2-trifluoroethanol; *U*, urea-denatured state; U_A, acid-denatured state.

One of the purposes of this paper is to examine the generality of existence of the compact denatured conformation. For this purpose we used an well-characterized globular protein, horse apomyoglobin.

Myoglobin is a small compact globular protein that contains no disulfide bond and has a unique monomeric form in solution whose three-dimensional structure is well resolved (Takano, 1977a, 1977b; Evans & Brayer, 1988). Removal of a heme molecule significantly decreases its stability but does not essentially change its structure; apomyoglobin (apoMb) is still compact, retains an ordered hydrophobic core, and has extensive helicity and a unique cooperative structure (Griko et al., 1988; Cocco et al., 1992; Eliezer & Wright, 1996). Thus, apoMb is a good model as a globular protein for equilibrium studies of denatured states. The conformational properties of apoMb have also been studied extensively in connection with the mechanism of protein folding (Jennings & Wright, 1993; Griko & Privalov, 1994; Eliezer et al., 1995; Gilmanshin et al., 1998). The detail of the pH and salt-induced conformational transitions were characterized (Barrick & Baldwin, 1993a; Goto & Fink, 1990; Nishii et al., 1994, 1995), and the structures of the denatured states found during these transitions have been extensively studied (Barrick & Baldwin, 1993b; Hughson et al., 1990; Kataoka et al., 1995; Loh et al., 1995; Eliezer et al., 1998). However, only a few detailed studies of the conformational transition in aqueous alcohol solution have been made. In the present study, we investigate details of the methanol-induced conformational transitions of horse heart apomyoglobin by a combined use of far- and near-UV CD, NMR spectroscopy, and small-angle X-ray scattering (SAXS), and construct a phase diagram as a function of pH and the methanol concentration.

The fact that the denatured state in high concentration of alcohols (*H*) has helical conformations and disrupted tertiary structures is widely accepted (Nelson & Kallenbach, 1986, 1989; Lehrman et al., 1990; Segawa et al., 1991; Dyson et al., 1992a, 1992b; Kippen et al., 1994; Shiraki et al., 1995; Hirota et al., 1997, 1998). However, there are not enough data to form general conclusions about the overall chain conformation (e.g., the size, the shape, etc.) of the *H* state (Kamatari et al., 1996, 1998; Hoshino et al., 1997). The difference between the *H* and "molten globule" states is also not clear because of the lack of such information. The second purpose of this paper is to investigate general features of the overall chain conformation of the *H* state. For this purpose, we used not only apoMb but also various other proteins that include ubiquitin, ribonuclease A, α-lactalbumin, β-lactoglobulin, and *Streptomyces* subtilisin inhibitor (SSI). Data from all of these in 60% methanol showed that they have expanded helical conformations and indicate the general existence of a considerably expanded and flexible broken rod-like chain conformation. To check the validity of this model in high concentration of methanol, we computer-simulated SAXS data using conformations that have helix regions connected by random chains. The qualitative agreement of the simulated SAXS data with the experimental data also supports this structural feature of the *H* state.

Results

The methanol-induced conformational transition of apoMb as monitored by far- and near-UV CD spectroscopy

Methanol-induced conformational transitions of apoMb were monitored first by far- and near-UV CD spectroscopy at various pH values. Figure 1 shows CD spectra in various concentrations of methanol at pH 5.4. The spectral changes induced by methanol at pH 2.0 and 5.4 are represented by ellipticity changes at 222 nm ($[\theta]_{222}$) and at 295 nm ($[\theta]_{295}$) as functions of methanol concentration in Figure 2, in which the former primarily reflects the secondary structure, especially the helical structure, whereas the latter reflects the tertiary structure. The pH value of 2.0 was selected as a typical condition producing the acid-denatured state in water, and pH 5.4 was selected as typical conditions for producing the native state from the phase diagram (Goto & Fink, 1990; Barrick & Baldwin, 1993a).

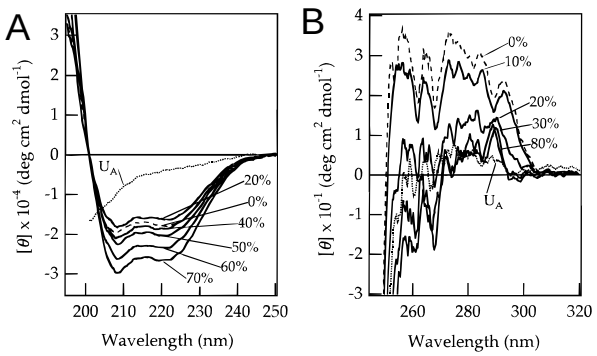

Fig. 1. A: Far-UV CD spectra of apoMb at pH 5.4 in 0% (------), 20% (—), 40% (—), 50% (—), 60% (—), and 70% (—) methanol. **B:** Near-UV CD spectra of apoMb at pH 5.4 in 0% (------), 10% (—), 20% (—), 30% (—), and 80% (—) methanol. For comparison, the spectrum for the acid-denatured (U_A: ------) state at pH 2.0 in water is presented. The spectra were measured at 25 °C with a fixed protein concentration of 60 μM.

At pH 2.0, addition of methanol decreased the $[\theta]_{222}$ value almost linearly over the full range of methanol concentration examined, suggesting that the transition is not a highly cooperative one (Fig. 2A). No significant change was observed for $[\theta]_{295}$ either, indicating that methanol did not induce any specific tertiary structure (Fig. 2B). Thus, we may conclude that, although the extent of secondary structure increases gradually, the protein continues to remain in a denatured state over the entire range of methanol concentration.

At pH 5.4, the behavior in the presence of methanol was completely different from that at pH 2.0. In the methanol concentration range from 0 to 30%, the $[\theta]_{222}$ value was almost constant and the $[\theta]_{295}$ value considerably decreased. The result indicates that the helical content does not change, but that almost all the tertiary structure is destroyed at 30% methanol. Above 40% methanol, the $[\theta]_{222}$ value decreased almost linearly with the concentration of methanol, suggesting a gradual formation of a helical structure.

The methanol-induced conformational transition of apoMb as monitored by ^{1}H-NMR spectroscopy

The methanol-induced conformational transition was also monitored by ^{1}H-NMR spectroscopy. The NMR experiments carried out in $^2H_2O/C^2H_3O^2H$ at pH* 5.6 are shown in Figure 3. At 0% methanol, the spectrum showed a considerable signal dispersion characteristic of the native conformation. Addition of methanol induced a gradual decrease of the signal intensities of the native species without significant changes in their chemical shifts, and all of the native signals disappeared at about 30% methanol. In the methanol concentration range from 20 to 30%, the signal disper-

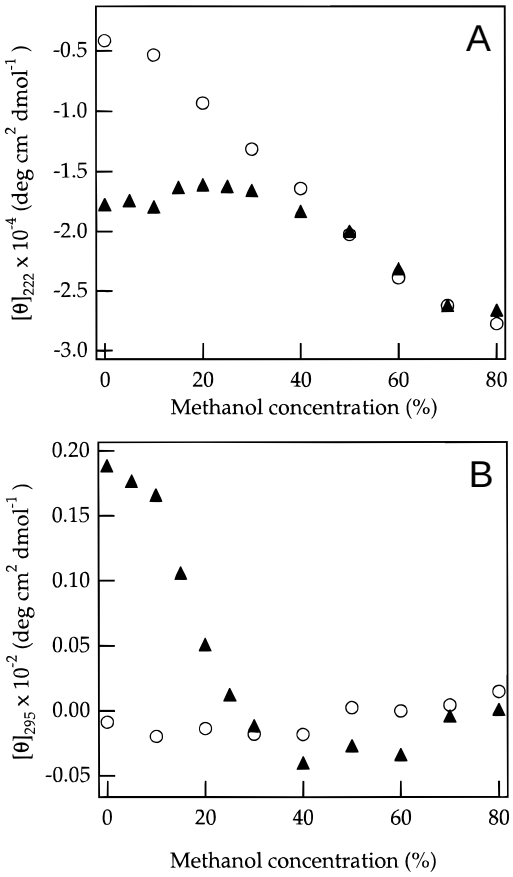

Fig. 2. Changes in ellipticity of apoMb with methanol concentration at pH 2.0 (open circles) and 5.4 (filled triangles): (**A**) at 222 nm; (**B**) at 295 nm. CD measurements were made at fixed concentration of apoMb (60 μM) at 25 °C.

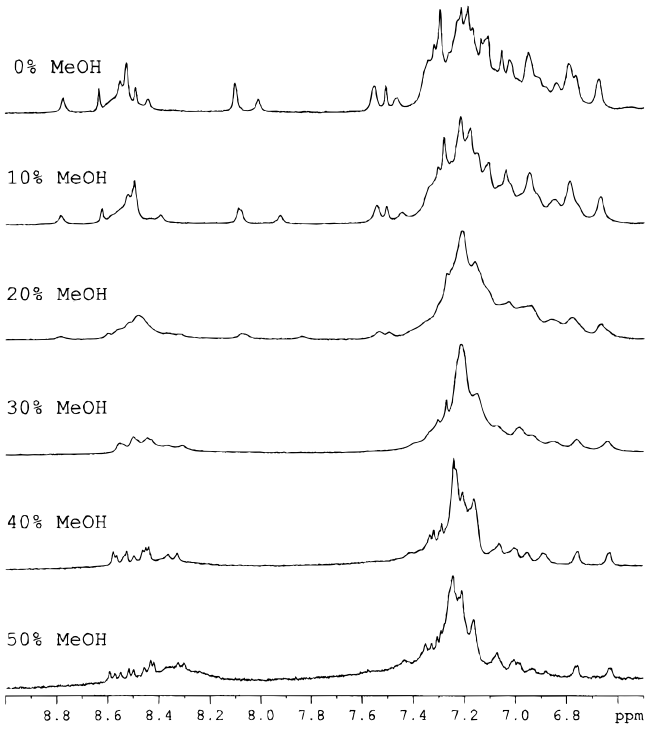

Fig. 3. The methanol concentration dependence of ^{1}H-NMR spectra of apoMb in $^2H_2O/C^2H_3O^2H$, at pH* 5.6 and 25 °C measured at 750 MHz. The methanol concentrations shown in the left-hand side of each spectrum. The protein concentrations was fixed at 0.4 mM throughout the experiments.

sion was almost lost, indicating that the tertiary structure was destroyed. The signals in 20 to 30% methanol were quite broad, resembling those of typical molten globule states induced by acid or salt. Above 40% methanol, the linewidth of the spectra gradually became sharp.

Phase diagram of apoMb involving N, U_A, I_M, and H conformations against pH and the methanol concentration

The results presented so far show the existence of at least one intermediate state in the methanol-induced conformational transition of apoMb. We call this intermediate state I_M. Therefore, apoMb exists in at least four typical conformational states, *N*, U_A (the acid denatured state), I_M, and *H* (the helical denatured state in the high concentration of methanol) in the water/methanol solvent mixture. The relative stability of these conformational states depends critically on pH and the methanol concentration. To make clear the dependence of the conformation on pH and methanol concentration, we studied both methanol-induced transitions at fixed pH and pH-induced transitions at fixed methanol concentrations. Above pH 6, precipitation of the protein prevents these measurements. The results are summarized in a phase diagram in Figure 4. We note that the midpoint between *N* and I_M depends on pH, but the midpoint between I_M (or U_A) and *H* mainly depends on the methanol concentration.

Chain conformations of apoMb in methanol/water as monitored by small-angle X-ray scattering

Small-angle X-ray scattering (SAXS) would be the best available technique for elucidating compactness and shape of proteins (Flanagan et al., 1992, 1993; Kataoka et al., 1993, 1994, 1995, 1997; Lattman, 1994; Konno et al., 1995, 1997; Kataoka & Goto, 1996). More specifically, Guinier plots of SAXS data give the radius of gyration (R_g), which provides information about the size or compactness. Figure 5A shows Guinier plots of SAXS data obtained for apoMb at infinite dilution under typical solvent conditions. Each curve in Figure 5A clearly possesses a region where the plot is well approximated by a straight line, the Guinier region (Guinier & Fournet, 1955). R_g values were deduced from the slopes of the regression lines within the Guinier region, defined as $R_gQ < 1.3$ in the present study (Kataoka et al., 1995), and are given in Table 1 for typical conformational states of apoMb. The R_g value of 22.7 Å for the I_M state is significantly smaller than 34.2 Å for the urea-denatured state or 30.2 Å for the acid-denatured state, and is closer to 19.7 Å for the native state or 23.1 Å for the molten globule state. The R_g value of 30.6 Å for the *H* state is significantly larger than that for the native state, but is closer to that for the urea- and acid-denatured states.

The Kratky plot, $I(Q)Q^2$ vs. *Q*, is useful for examining the globularity or randomness of a chain molecule (Glatter & Kratky, 1982), and has been widely used to study folding intermediates and the structures of non-native states of proteins (Damaschun et al., 1991, 1993; Flanagan et al., 1993; Kataoka et al., 1993, 1995; Kataoka & Goto, 1996). It gives a clear peak for the globular

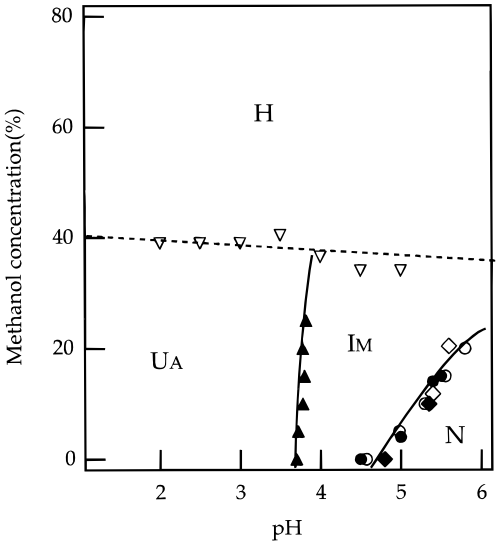

Fig. 4. Experimentally determined phase diagram of apoMb in H_2O/CH_3OH mixture at 25 °C. *N*, the native state; U_A, the acid-denatured state; I_M, the compact denatured (or molten globule) state; *H*, the helical denatured state. The continuous lines were drawn to indicate the phases boundary where the fractions of the two conformational states are equal. The broken line indicates the midpoint of $[\theta]_{222}$ values between the denatured state in 0 and 80% methanol. Each data point was obtained from a titration. Open symbols were obtained in an experiment in which the methanol concentration was varied at fixed pH values and filled symbols were obtained in an experiments in which pH values varied at fixed methanol concentration. The symbols of open circles and closed circles are obtained by $[\theta]_{295}$ values. The symbols of open diamonds and closed diamonds are obtained by NMR spectroscopy. The symbol down open triangle and up closed triangle is obtained by $[\theta]_{222}$ and $[\theta]_{290}$ values, respectively. Data above pH 4.5 could not be obtained due to precipitation of the protein.

conformation, while it shows a plateau and then increases monotonically for the unfolded chain-like conformation (Flanagan et al., 1993; Kataoka et al., 1993; Kataoka & Goto, 1996). Figure 5B shows the Kratky plots for the typical conformational states of apoMb. The plots for the I_M and *H* states show that the conformations are globular and expanded, respectively. We find that the plots for the I_M and *H* state are quite similar to those for the molten globule and acid-denatured state, respectively.

Structure of the H state of proteins

We also investigated the structure of other proteins, ubiquitin, ribonuclease A, α-lactalbumin, β-lactoglobulin, and *Streptomyces* subtilisin inhibitor (SSI) in 60% methanol at pH 2. All of these have a helical content higher than that of the native state monitored by far-UV CD spectroscopy (data not shown), no specific tertiary structure monitored by near-UV CD and NMR spectroscopy (data not shown) and a 1.5–2.0-fold expansion (Table 2) with chain-like conformations (Fig. 6; Table 2) as monitored by SAXS.

Computer simulation of the SAXS data

To examine structural features of the *H* state, we performed computer simulation of SAXS data of cytochrome *c*. Because, at present, we do not have the structural information at the atomic level on the *H* state, we generated a structural model in which the helical regions in the native state remain helical and the remainder of the protein adopts a random coil conformation. We call this model for simulation a broken helix (*BH*). Generating many conformations of the *BH* chain and taking correct account of the contrast effect of solvent water on X-ray scattering, we obtained their scattering profiles.

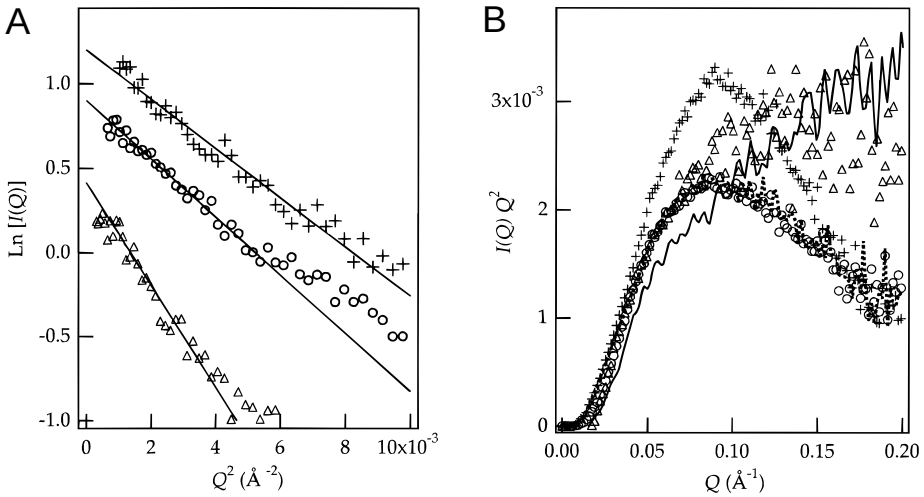

Fig. 5. A: Guinier plots for apoMb in the I_M (open circles), *H* (open triangles), and native (+) states at 25 °C. Each plot was obtained by extrapolation of the data for four different protein concentrations to zero protein concentration (Kataoka et al., 1989). The experimental conditions were as follows: pH 4.5 in 15% methanol for the I_M state; pH 2.0 in 60% methanol for the *H* state; pH 7 in water for *N* state. For clarity, individual plots are shifted on the $\ln[I(Q)]$ axis. The regression lines were fitted to the data within $R_gQ < 1.3$. **B:** Kratky profiles of apoMb in the I_M (open circles), *H* (open triangles), native (+), molten globule (------), acid-denatured (——) states at 25 °C. The experimental conditions were as follows: pH 4.5 in 15% methanol for the I_M state; pH 2.0 in 60% methanol for the *H* state; pH 7 in water for the *N* state; pH 4 in water for the molten globule state; pH 2.0 in water for the acid-denatured state. The protein concentration was kept at 10 mg/mL for all the profiles.

Table 1. *Spectroscopic properties of typical conformational state of apoMb*[a]

Conformational states	$[\theta]_{222}$	$[\theta]_{295}$	Chemical shift dispersion[b]	Linewidth[c]	R_g (Å)	Shape[d]
I_M	−16.000	−2	Small	Broad	22.7	Globular
H	−23.000	0	Small	Very sharp	30.6	Chain
N	−18.000	20	Large	Sharp	19.7[e]	Globular
U_A	−4.000	0	Small	Sharp	30.2[e]	Chain
MG	−16.000	0	Small	Broad	23.1[e]	Globular
U	−1.000	−1	Small	Very sharp	34.2[e]	Chain

[a]Experimental conditions were as follows: pH 4.5 and 15% methanol for the I_M state (I_M); pH 2 and 60% methanol for the helical denatured state (H); pH 5.5 in water for the native state (N); pH 2 in water for the acid-denatured state (U_A); pH 2 and 20 mM NaTCA for the TCA-induced molten globule state (MG); pH 2 and 5 M urea for the urea-denatured state (U) at 25 °C.
[b]Chemical shifts dispersion of ^{1}H-NMR spectra.
[c]Linewidth of ^{1}H-NMR signals.
[d]Molecular shape obtained from Kratky plots.
[e]Kataoka et al. (1995).

A Kratky plot of the scattering profile for the *BH* model, as determined from the average of those calculated above, is shown in Figure 7B. For comparison, simulated Kratky plots for the native and the random coil (RC) structures are also displayed in the figure. The simulated Kratky plot for the native state exhibits a large peak at $Q = 0.12$ Å^{-1}, characteristic of the globular structure, whereas the plot for the random coil chain reaches a plateau, both of which agree with theoretical expectations. The simulated Kratky plot for the *BH* chain does not have a clear peak, and qualitatively agrees with experimental data for the *H* chain. The R_g values for the native, RC, and *BH* model obtained from the simulation are 13.5, 31.5, and 29.8 Å, respectively. These values are also consistent with the experimental data (Table 2; Kamatari et al., 1996). These results support the view that the *H* state has an expanded *BH*-like structure.

Discussion

Conformational transitions of apoMb in methanol–water solvent

Existence of an intermediate state (I_M)

We investigated details of the transition of horse heart apomyoglobin (apoMb) by a combined use of far- and near-UV CD and NMR spectroscopy and small-angle X-ray scattering (SAXS). The discrepancy of the transitions monitored by far and near-UV CD spectroscopy (Fig. 2) and characteristic NMR spectra in about 30% methanol, which are quite distinct from that of the native state and that found in the methanol concentration above 50% (Fig. 3), show the existence of at least one intermediate state (I_M) in the methanol-induced conformational transition. Therefore, apoMb ex-

Table 2. *R_g of the H, native (N), and urea-denatured (U) states of proteins*[a]

	MW	R_{g_H}	R_{g_N}	R_{g_U}	R_{g_H}/R_{g_N}	Shape of the H state[b]
Ubiquitin	8.600	28.4	13.2	26.3	2.2	Chain
Cytochrome c[c]	12.400	31.7	14.6	32.1	2.2	Chain
Ribonuclease A	13.700	25.3	15.0[d]	27.3	1.7	Chain
Lysozyme[e]	14.300	24.9	15.7	28.7	1.6	Chain
α-Lactalbumin	14.300	24.3	15.7[f]	30[f]	1.5	Chain
Apomyoglobin	17.500	30.6	19.7[g]	34.2[g]	1.6	Chain
β-Lactoglobulin	18.400	39.5	18.0	44.4	2.2	Chain
SSI	11.500	28.3	21.8[h] (dimer)	32[h]	—	Chain

[a]Experimental conditions were as follows: pH 2 in 60% methanol for the *H* state at 25 °C; pH 7 in 50 mM Tris-HCl buffer for the *N* state of ubiquitin at 25 °C; pH 4.5 in water for the *N* state of cytochrome *c* at 25 °C; pH 5.7 in water for the *N* state of ribonuclease A at 56 °C; pH 7 in water for the *N* state of lysozyme, and α-lactalbumin at 25 °C; pH 6 in 10 mM HEPES buffer for the *N* state of apomyoglobin at 20 °C; pH 7.0 in water for the *N* state SSI at 20 °C; pH 2 in water for the *N* state of α-lactoglobulin at 25 °C; pH 2 in 5 M urea for the *U* state of ubiquitin, cytochrome *c*, ribonuclease A, lysozyme, α-lactalbumin, and β-lactoglobulin at 25 °C; pH 2 in 5 M urea for the *U* state of apomyoglobin at 20 °C; pH 3.0 in 5 M urea for the *U* state of SSI at 20 °C.
[b]Molecular shape obtained from Kratky plots.
[c]Kamatari et al. (1996).
[d]Sosnick and Trewhella (1992).
[e]Kamatari et al. (1998).
[f]Kataoka et al. (1997).
[g]Kataoka et al. (1995).
[h]Konno et al. (1995).

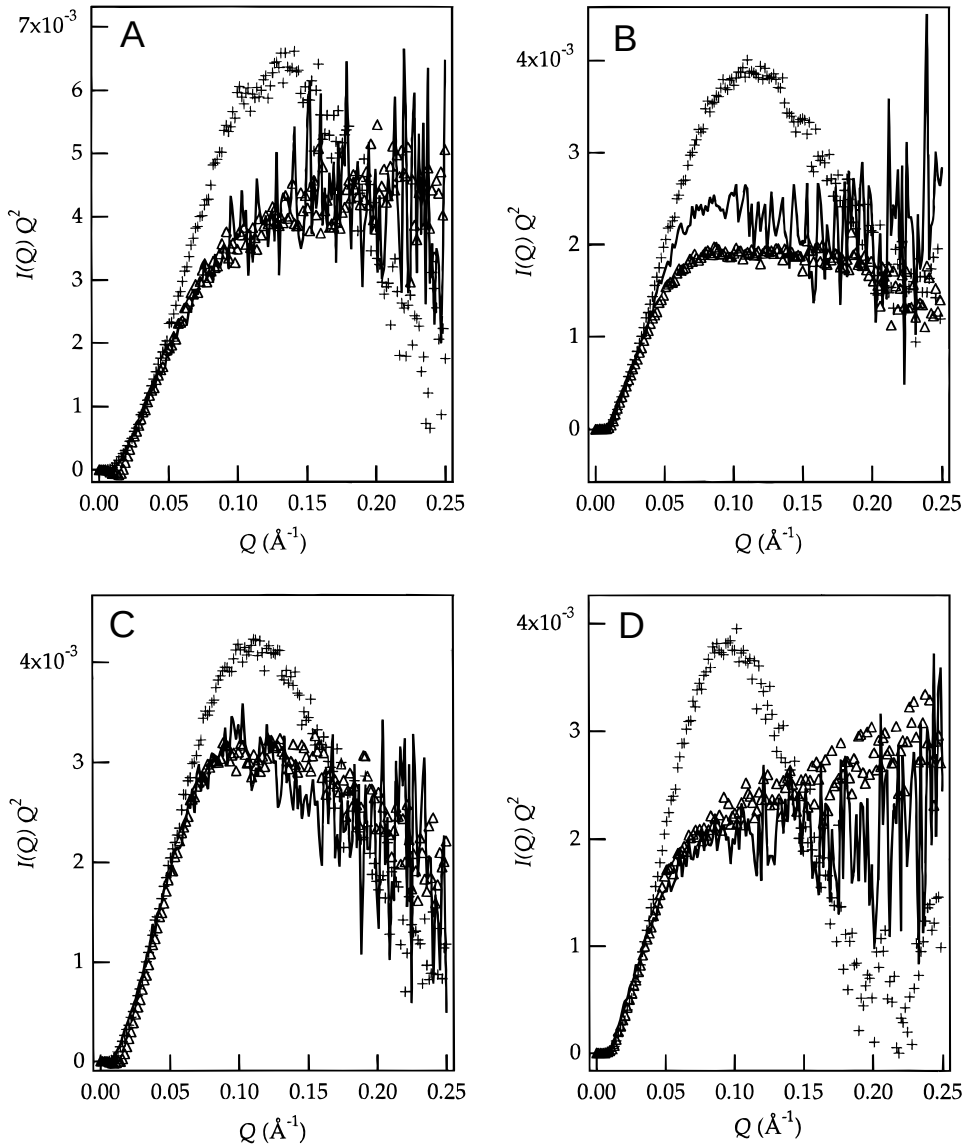

Fig. 6. Kratky profiles of (**A**) ubiquitin, (**B**) ribonuclease A, (**C**) α-lactalbumin, and (**D**) β-lactoglobulin in the *H* (open triangles), native (+), urea-denatured (—) states at 25 °C. The experimental conditions were as follows: pH 2.0 in 60% methanol for the *H* state; pH 7 in water for the *N* state of ubiquitin, ribonuclease A, and α-lactalbumin; pH 2 in water for the *N* state of β-lactoglobulin; pH 2 in water containing 5 mM urea for the urea-denatured state. The protein concentration was kept at 10 mg/mL for all the profiles.

ists in at least four typical conformational states, *N*, U_A (the acid denatured state), I_M, and *H* (the helical denatured state in the high concentration of methanol) in water/methanol solvent.

Structure of the I_M state

This intermediate state has a helical content similar to that of the native state as monitored by far-UV CD spectroscopy (Fig. 2A), no specific tertiary structure as monitored both by near-UV CD (Fig. 2B) and NMR spectroscopy (Fig. 3), and a compact (Table 1) and globular (Fig. 5B) conformation as monitored by SAXS. All the available structural information indicates that the structure of the I_M is almost identical with that of the well-known molten globule state (*MG*) of this protein induced by acid or salt (Barrick & Baldwin, 1993a, 1993b; Nishii et al., 1994, 1995; Kataoka et al., 1995).

Structure of the H state

The *H* state of apoMb has a helical content higher than that of the native state as monitored by far-UV CD spectroscopy (Figs. 1A, 2A), no specific tertiary structure as monitored both by near-UV CD (Figs. 1B, 2B) and NMR spectroscopy (Fig. 3), and an expanded (Table 1) and nonglobular (Fig. 5B) conformation as monitored by SAXS. Taking all these results together, we conclude that the *H* state of apoMb has a considerably expanded and chain-like conformation with an extremely high helical content.

Phase diagram

To make clear the dependence of the conformations on pH and methanol concentration, we constructed a phase diagram as a function of pH and the methanol concentration (Fig. 4). The phase diagram indicates that the compact denatured state (I_M or *MG*) is

stable under relatively mild denaturing conditions, whereas the expanded denatured states (U_A and H) are realized under extreme conditions of pH (large electric repulsion) or alcohol concentration (small hydrophobic interactions).

It is known that non-native states of protein can exist in living cells and can be involved in a number of physiological processes (Bychkova et al., 1988). The *MG* state is one of the candidate structure for the non-native state in the living cell. It has been suggested that a local decrease of pH and a decrease of the dielectric constant of the bulk solvent on the membrane surface can be responsible for the denaturation of proteins (Bychkova et al., 1988; van der Goot et al., 1991; Bychkova & Ptitsyn, 1993; Ptitsyn et al., 1995), and the suggestion has been confirmed for cytochrome *c* (Bychkova et al., 1996; Kamatari et al., 1996) and β-lactoglobulin (Uversky et al., 1997). The phase diagram of the apoMb (Fig. 4) shows the existence of the *MG* state under such conditions and further support the suggestion.

General existence of the compact denatured conformations in alcohol–water mixtures

This feature of the transition of apoMb is similar to that of cytochrome *c* (Bychkova et al., 1996; Kamatari et al., 1996), in which the compact denatured state appears and makes a striking contrast to that of lysozyme (Hoshino et al., 1997; Kamatari et al., 1998) for which the transition is highly cooperative. Comparison of the phase diagram of apoMb (Fig. 4), cytochrome *c* (Kamatari et al., 1996), and lysozyme (Kamatari et al., 1998) indicates that the region for the I_M state of the apoMb is much wider than those of cytochrome *c* and lysozyme, showing that the stability of the I_M state is highly protein dependent. The area of the I_M state in the phase diagram decreases in the order apoMb > cytochrome *c* > lysozyme. Similar cooperativity differences have also been observed in other denaturation processes. For example, in the case of acid denaturation, the compact denatured state of apomyoglobin appears not only in high salt and acidic conditions but also at intermediate pH (about pH 4; Goto & Fink, 1990; Barrick & Baldwin, 1993a); that of cytochrome *c* appears only in high salt and acidic condition (Ohgushi & Wada, 1983); that of lysozyme does not appear at all (Tanford, 1970; Khechinashvili et al., 1973; Haezebrouck et al., 1995). One reasonable explanation of the difference in these feature of the transitions may be that these three states, the native (*N*), compact denatured (*MG*), and expanded (*U* and *H*) states, are general thermodynamic states not only in the pH–salt concentration plane but also in the alcohol–water plane, and that the *N*, *MG*, and *U* states are brought into existence by the balance of their relative stability. Increasing stability of the *N* state or decreasing stability of the *MG* state of lysozyme should be responsible for the cooperative transition without appearance of the *MG* state.

The existence of a compact denatured state in the methanol–water solvent mixture has been reported for various proteins, which include cytochrome *c* (Bychkova et al., 1996; Kamatari et al., 1996), β-lactoglobulin (Uversky et al., 1997), and apoMb (the present study). The compact denatured state of β-lactoglobulin was reported not only in methanol but also in several types of organic solvents including ethanol, isopropanol, dimethylformamide, and dioxane (Uversky et al., 1997). The compact denatured state in hexafluoroacetone hydrate was also reported for lysozyme (Bhattacharjya & Balaram, 1997). There results also indicate the general existence of the *MG* state in alcohol–water solvents.

General feature of the expanded conformation (H) in high concentrations of alcohol

The highly helical conformation and disrupted tertiary structure of proteins in alcohol are widely known, but their size and overall shape are not known until recently (Kamatari et al., 1996, 1998; Hoshino et al., 1997). We investigated the general feature of the *H* structure using not only apoMb but also several other proteins,

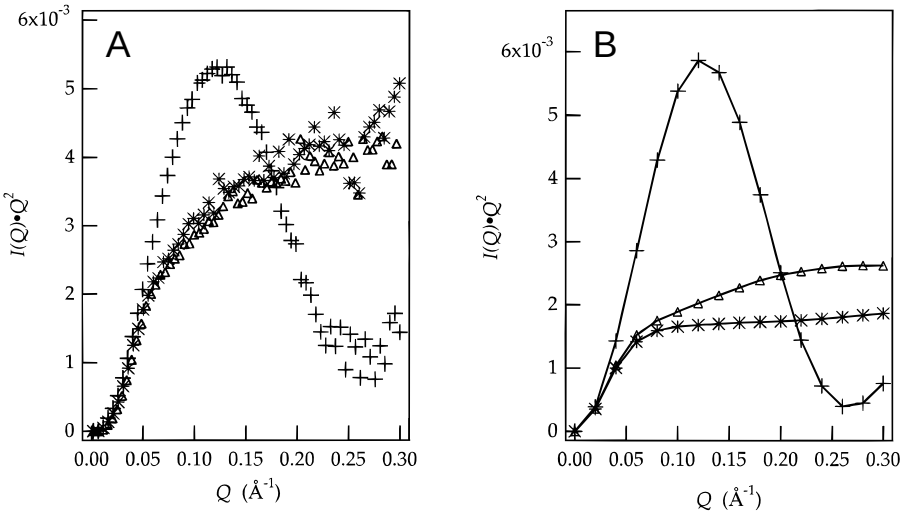

Fig. 7. A: Experimental Kratky profiles of cytochrome *c* in the native (+), *H* (open triangles), and acid-denatured (*) states at 25 °C. The experimental conditions were as follows: pH 4.5 for the native state; pH 1.7 and 60% methanol for *H*; pH 2.0 for the acid-denatured state. The protein concentrations were kept at 10 mg/mL for all the profiles. **B:** Simulated Kratky profiles of cytochrome *c* in the native (+), broken helix in which protein have native helical elements but the other regions are random coil conformations (open triangles), and random coil (*) states.

which include ubiquitin, ribonuclease A, α-lactalbumin, β-lactoglobulin, and *Streptomyces* subtilisin inhibitor (SSI). The R_g values are summarized in Table 2. This is quite a range of proteins. ApoMb and cytochrome *c* are α-proteins; ubiquitin, ribonuclease A, lysozyme, α-lactalbumin, and *Streptomyces* subtilisin inhibitor (SSI) are α/β-proteins; and β-lactoglobulin is a β-rich protein. SSI is a dimer protein, while the others are monomeric. However, all of the R_g values of the *H* state are expanded 1.5–2.2-fold compared to those of the native states, and are close to that of the urea-denatured states (Table 2). In all cases the Kratky patterns also indicated nonglobular conformations (Fig. 5B).

A 2,2,2-trifluoroethanol (TFE)-induced highly helical structure of lysozyme has been extensively studied by Buck and coworkers by NMR methods (Buck et al., 1993, 1995, 1996), who showed that the protein has six helices, five of which are located in the helical region while the other is located in the β-sheet region of the native state. More recently Brutscher and coworkers reported the NMR characterization of the ubiquitin in 60% methanol/40% water at pH 2, conditions identical to ours (Brutscher et al., 1997). They showed that the N-terminal half of the *H* state, comprising the antiparallel β-sheet and a central α-helix, conserve the native secondary structural elements while the C-terminal half, which is in the native state rich in β-strand character, undergoes a methanol-induced transition to a dynamic state with a uniformly high propensity for helical structure. They also showed there three segment (one β-sheet and two α-helix) have independent rotational correlation time. Combining these results with ours, we suppose that the *H* states have expanded and flexible broken rod-like chain conformations, in which the rods are usually helical but may be small sets of β-strands on rare occasions.

The fact that *H* states have expanded conformations is also supported by other data in addition to the SAXS results shown above. One example is the qualitative agreement of the experimental and simulated Kratky plots in which protein have native helical elements with other regions in random coil conformations (Fig. 7). This also supports the validity of our *H* conformation model. The absence of fluorescence quenching of the *H* state of cytochrome *c* (Kamatari et al., 1996) also supports the expanded conformation. Horse cytochrome *c* has a single tryptophan residue, Trp59, which is completely buried near the center of the molecule and hydrogen bonded to a heme propionate. In the native and molten globule state of this protein, the fluorescence of Trp59 is quenched due to resonance energy transfer to the heme moiety. On the other hand, both the *H* and acid-denatured states show an increased level of fluorescence intensity, reflecting a separation of Trp59 from the heme moiety. Absence of the hydrophobic core of the *H* state, indicated by the absence of ANS binding (Alexandrescu et al., 1994; Kamatari et al., 1998), and noncooperative heat denaturation (Buck et al., 1993) may also indirectly support the expanded conformation of the *H* state.

Hoshino et al. reported the TFE-denatured state of lysozyme (Hoshino et al., 1997). Their data show that the denatured state in 30% TFE has a similar R_g value and chain shape to the GdnHCl-denatured state rather than the native state. This indicates that the noncompact nonglobular conformation exists not only in methanol–water solvents but also in the other alcohol–water solvents.

In conclusion, the helical and noncompact conformation (*H*) in an alcohol-rich aqueous environment should be a general conformation in globular proteins. This structure is clearly distinguishable from the "molten globule" type of compact denatured state.

Conclusions

Taking all the results together, the compact and expanded conformations formed in alcohol–water mixtures appear to be general conformational states. These conformations are clearly distinguishable by their size, shape, and existence of hydrophobic clustering. The present study also indicates that the compact denatured state (I_M or *MG*) is stable under relatively mild denaturing conditions, whereas the expanded denatured states (U_A or *H*) are realized under extreme conditions of pH (large electric repulsion) or the concentration of alcohol (small hydrophobic interactions).

Materials and methods

Materials

ApoMb was prepared from horse heart myoglobin (Sigma Type IV) by 2-butanone extraction of the heme (Hapner et al., 1968), and purified by Sepadex G-50 filtration to remove aggregates. Hen egg white lysozyme (Sigma, St. Louis, Missouri), bovine ubiquitin (Sigma), horse heart cytochrome *c* (type VI; Sigma), bovine pancreatic ribonuclease A (type XII-A; Sigma), α-lactalbumin (Sigma), and β-lactoglobulin (Sigma) were used without further purification. Crude solutions of SSI were obtained from *Streptomyces albogriseolus* S-3253, and were purified on chromatographic columns with DE52 (Watman, Maidstone, UK) and Sephacryl S-200 (Pharmacia, Uppsala, Sweden), as described by Saito and Murao (1973). The homogeneity of the proteins was checked by electrophoresis. The concentration of apoMb in solutions was determined photometrically, using $\epsilon_{280} = 14{,}300$ (Crumpton & Polson, 1965). Methanol concentrations are given as %, v/v.

Methods

pH measurements

The pH of the solution was measured on a HORIBA pH/ion meter F-23. The pH values of the protein solutions in H_2O/CH_3OH were adjusted by adding HCl. The pH values in ^2H_2O/$C^2H_3O^2H$ solvent were adjusted by adding ^{2}HCl and are given as pH*. The reported pH and pH* values are direct meter readings uncorrected for the isotope and methanol effects.

CD measurements

CD measurements were carried out at 25 °C on a Jasco spectropolarimeter, Model J-720, with a quartz cell of 0.1 mm light path for the far-UV and of 10.0 mm light path for the near-UV CD region at protein concentrations of 60 μM. The temperature of the cell was controlled by circulating water through a jacket around the cell to within $\pm$0.1 °C. The results are expressed as mean residue ellipticity $[\theta]$, which is defined as $[\theta] = 100\ \theta_{obs}/lc$, where θ_{obs} is the observed ellipticity in degrees, *c* is the concentration in residue moles per liter, and *l* is the length of the light path in centimeters.

NMR measurements

NMR measurements were performed at 25 °C on a Bruker (Germany) DMX 750 NMR spectrometer operating at 750 MHz. The protein sample was dissolved in H_2O/CH_3OH or $^2H_2O/C^2H_3O^2H$ to a concentration of 1 to 7 mM with the sodium salt of 3-trimethyl-[3,3,2,2-^{2}H]-propionic acid (TSP) added as a internal chemical shift reference.

SAXS measurements

Solution X-ray scattering experiments were carried out at the solution scattering station (SAXS camera) installed at BL-10C, the Photon Factory, Tsukuba, Japan (Ueki et al., 1985; Kataoka et al., 1991). The sample to detector distance was about 90 cm for measurements of SAXS, calibrated with meridional diffraction of dried chicken collagen. The X-ray wavelength was 1.488 Å. The sample cell was 50 μL in volume with a 15 μm thick quartz window, and had a 1 mm X-ray path length. The temperature of the sample was controlled at 25 °C by circulating temperature-controlled water. Protein samples were dissolved in H_2O/CH_3OH; concentrations were varied within the range of 1 to 10 mg/mL, and for each experiment the measurement time was 10 min. Solvent solutions containing no protein sample were measured as background.

Analysis of SAXS data

The SAXS data were processed with both Macintosh (Apple) and PC9801 (NEC) personal computers. The scattering curve at infinite dilution was obtained from a series of scattering data with different protein concentrations (Kataoka et al., 1989). X-ray scattering intensities at the small-angle region are given as $I(Q) = I(0)\exp(-R_g^2Q^2/3)$, where Q and $I(0)$ are the momentum transfer and the intensity at 0 scattering angle, respectively (Glatter & Kratky, 1982). Q is defined by $Q = 4\pi \sin\theta/\lambda$, where 2θ and λ are the scattering angle and the X-ray wavelength, respectively. R_g can then be obtained from the slope of the Guinier plot, a plot of $\ln[I(Q)]$ against Q^2. No significant aggregation was observed in any measurement.

Computer simulation of SAXS data

About 300 conformations are generated for each of the two structural models of denatured cytochrome *c*: the random coil (*RC*) and the broken helix (*BH*). It is assumed in the *BH* model that the conformation of a helical segment in the native state is preserved with the same conformation and the other segments have a random-coil conformation. Random coil conformations in both the *RC* model and the *BH* model are generated as follows: dihedral angles for main and side chains of each amino acid residue are randomly chosen from the ensemble of dihedral-angle values determined from the atomic coordinate data of proteins in Protein Data Bank (PDB). This procedure is equivalent to sampling each dihedral angle in proportion to its probability distribution.

It is confirmed that using only 100 conformations in the calculation yields essentially the same general feature of the scattering profile as that for 300 conformations. So, the number of generated conformations, 300, are in practice large enough to give characteristic SAXS profiles of the two models. This will partly be due to the following situation: the scattering profile for each conformation is the average of those estimated for 160 chains, with the identical conformation and mutually different orientations to the direction of incident X-ray. Thus, the theoretical profile is obtained through a double process of conformational and orientational averagings. The number of orientations is chosen large enough to make the orientational averaging efficiently. The number 160 taken in our calculation corresponds to averaging over the hemispherical solid angle of 2π with a division of $2\pi/160 = 0.039$ sr (steradian).

X-ray scattering profiles are calculated for all the conformations generated, and the contrast effect of solvent water is incorporated by means of the modified version of the recently developed surface integration method. Averaging the calculated profiles yields a SAXS profile for each model of the denatured cytochrome *c*. Details of the SAXS simulation method will be reported elsewhere.

Acknowledgments

We are indebted to Y. Harano and H. Kamikubo for their help with X-ray scattering experiments. We thank Y. Inoko and K. Kobayashi for their support with experiments at the Photon Factory. The X-ray scattering measurements were performed under an approval from the Program Advisory Committee of the Photon Factory (Proposal Nos. 95G262 and 95G264). We thank Professor O.B. Ptitsyn, Dr. V.E. Bychkova, Dr. M. Buck, Dr. M. Hoshino, Dr. D. Hamada, Dr. R. Brueschweiler, Professor F. Toma, Dr. T. Yamaguchi, and Dr. J.A. Jones for their useful discussion. This work was supported by the Grant-in-Aid for Scientific Research (given to K.A.) and for JSPS Fellows (given to Y.O.K.) from the Ministry of Education, Science, Sports and Culture of Japan.

References

Alexandrescu AT, Ng YL, Dobson CM. 1994. Characterization of a trifluoroethanol induced partially folded state of α-lactalbumin. *J Mol Biol 235*:587–599.

Barrick D, Baldwin RL. 1993a. Three-state analysis of sperm whale apomyoglobin folding. *Biochemistry 32*:3790–3796.

Barrick D, Baldwin RL. 1993b. The molten globule intermediate of apomyoglobin and the process of protein folding. *Protein Sci 2*:869–876.

Bhattacharjya S, Balaram P. 1997. Hexafluoroacetone hydrate as a structure modifier in proteins: Characterization of a molten globule state of hen egg-white lysozyme. *Protein Sci 6*:1065–1073.

Brutscher B, Brüschweiler R, Ernst RR. 1997. Backbone dynamics and structural characterization of the partially folded A state of ubiquitin by ^{1}H, ^{13}C, and ^{15}N nuclear magnetic resonance spectroscopy. *Biochemistry 36*:13043–13053.

Buck M, Radford SE, Dobson CM. 1993. A partially folded state of hen egg white lysozyme in trifluoroethanol: Structural characterization and implications for protein folding. *Biochemistry 32*:667–678.

Buck M, Schwalbe H, Dobson CM. 1995. Characterization of conformational preferences in a partially folded protein by heteronuclear NMR spectroscopy: Assignment and secondary structure analysis of hen egg-white lysozyme in trifluoroethanol. *Biochemistry 34*:13219–13232.

Buck M, Schwalbe H, Dobson CM. 1996. Main-chain dynamics of a partially folded protein: ^{15}N NMR relaxation measurements of hen egg white lysozyme denatured in trifluoroethanol. *J Mol Biol 257*:669–683.

Bychkova VE, Dujsekina AE, Klenin SI, Tiktopulo EI, Uversky VN, Ptitsyn OB. 1996. Molten globule-like state of cytochrome *c* under conditions simulating those near the membrane surface. *Biochemistry 35*:6058–6063.

Bychkova VE, Pain RH, Ptitsyn OB. 1988. The "molten globule" state involved in the translocation of proteins across membrane? *FEBS Lett 238*:231–234.

Bychkova VE, Ptitsyn OB. 1993. The molten globule in vitro and in vivo. *Chemtracts Biochem Mol Biol 4*:133–163.

Cocco MJ, Kao Y, Phillips AT, Lecomte JTJ. 1992. Structural comparison of apomyoglobin and metaquomyoglobin: pH titration of histidines by NMR spectroscopy. *Biochemistry 31*:6481–6491.

Crumpton MJ, Polson A. 1965. A comparison of the conformation of sperm whale metmyoglobin with that of apomyoglobin. *J Mol Biol 11*:722–729.

Damaschun G, Damaschun H, Gast K, Gernat C, Zirwer D. 1991. Acid denatured apo-cytochrome *c* is a random coil: Evidence from small-angle X-ray scattering and dynamic light scattering. *Biochim Biophys Acta 1078*:289–295.

Damaschun G, Damaschun H, Gast K, Misselwitz R, Müller JJ, Pfeil W, Zirwer D. 1993. Cold denaturation-induced conformational changes in phosphoglycerate kinase from yeast. *Biochemistry 32*:7739–7746.

Dyson HJ, Merutka G, Waltho JP, Lerner RA, Wright PE. 1992a. Folding of peptide fragments comprising the complete sequence of proteins. Models for initiation of protein folding. I. Myohemerythrin. *J Mol Biol 226*:795–817.

Dyson HJ, Sayre JR, Merutka G, Shin HC, Lerner RA, Wright PE. 1992b. Folding of peptide fragments comprising the complete sequence of proteins. Models for initiation of protein folding. I. Plastocyanin. *J Mol Biol 226*:819–835.

Eliezer D, Jennings PA, Wright PE, Doniach S, Hodgson KO, Tsuruta H. 1995. The radius of gyration of an apomyoglobin folding intermediate. *Science 270*:487–488.

Eliezer D, Wright PE. 1996. Is apomyoglobin a molten globule? Structural characterization by NMR. *J Mol Biol 263*:531–538.

Eliezer D, Yao J, Dyson HJ, Wright PE. 1998. Structural and dynamic characterization of partially folded states of apomyoglobin and implications for protein folding. *Nat Struct Biol 5*:148–155.

Evans SV, Brayer GD. 1988. Horse heart metmyoglobin. A 2.8-A resolution three-dimensional structure determination. *J Mol Biol 263*:4263–4268.

Flanagan JM, Kataoka M, Fujisawa T, Engelman DM. 1993. Mutation can cause large changes in the conformation of a denatured protein. *Biochemistry 32*:10359–10370.

Flanagan JM, Kataoka M, Shortle D, Engelman DM. 1992. Truncated staphylococcal nuclease is compact but disordered. *Proc Natl Acad Sci USA 89*:748–752.

Gilmanshin R, Callendar RH, Dyer RB. 1998. The core of apomyoglobin E-form folds at the diffusion limit. *Nat Struct Biol 5*:363–365.

Glatter O, Kratky O. 1982. *Small angle X-ray scattering*. New York: Academic Press.

Goto Y, Fink AL. 1990. Phase diagram for acidic conformational states of apomyoglobin. *J Mol Biol 214*:803–805.

Griko YV, Privalov PL. 1994. Thermodynamic puzzle of apomyoglobin unfolding. *J Mol Biol 202*:127–138.

Griko YV, Privalov PL, Venyaminov YS, Kutyshenko VP. 1988. Thermodynamic study of the apomyoglobin structure. *J Mol Biol 202*:127–138.

Guinier A, Fournet B. 1955. *Small-angle scattering of X-rays*. New York: John Wiley.

Haezebrouck P, Joniau M, Dael HV, Hooke SD, Woodruff ND, Dobson CM. 1995. An equilibrium partially folded state of human lysozyme at low pH. *J Mol Biol 246*:382–387.

Hapner KD, Bradshaw RA, Hartzell CR, Gurd FRN. 1968. Comparison of myoglobin form harbor seal, porpoise, and sperm whale. I. Preparation and characterization. *J Biol Chem 243*:683–689.

Hirota N, Mizuno K, Goto Y. 1997. Cooperative α-helix formation of β-lactoglobulin and melittin induced by hexafluoroisopropanol. *Protein Sci 6*:416–421.

Hirota N, Mizuno K, Goto Y. 1998. Group additive contributions to the alcohol-induced α-helix formation of melittin: Implication for the mechanism of the alcohol effects on proteins. *J Mol Biol 275*:365–378.

Hoshino M, Hagihara Y, Hamada D, Kataoka M, Goto Y. 1997. Trifluoroethanol-induced conformational transition of hen egg-white lysozyme studied by small-angle X-ray scattering. *FEBS Lett 416*:72–76.

Hughson F, Wright P, Baldwin R. 1990. Structural characterization of a partly folded apomyoglobin intermediate. *Science 249*:1544–1548.

Jennings PA, Wright PE. 1993. Formation of a molten globule intermediate early in the kinetic folding pathway of apomyoglobin. *Science 262*:892–896.

Kamatari YO, Konno T, Kataoka M, Akasaka K. 1996. The methanol-induced globular and expanded denatured states of cytochrome *c*: A study by CD, fluorescence, NMR and small-angle X-ray scattering. *J Mol Biol 259*:512–523.

Kamatari YO, Konno T, Kataoka M, Akasaka K. 1998. The methanol-induced transition and the expanded helical conformation of lysozyme. *Protein Sci 7*:681–688.

Kataoka M, Flanagan JM, Tokunaga F, Engelman DM. 1994. Use of X-ray solution scattering for protein folding study. In: Chance B, Deisenhofer J, Ebashi S, Goodhead DT, Helliwell JR, Huxley HE, Iizuka T, Kirz J, Mitsui T, Rubenstein E, Sakabe N, Sasaki T, Schmahl G, Stuhrmann HB, Wüthrich K, Zaccai G, eds. *Synchrotron radiation in the biosciences.* Oxford: Clarendon Press. pp 187–194.

Kataoka M, Goto Y. 1996. X-ray solution scattering studies of protein folding. *Folding Design 1*:R107–R114.

Kataoka M, Hagihara Y, Mihara K, Goto Y. 1993. Molten globule of cytochrome *c* studied by the small angle X-ray scattering. *J Mol Biol 229*:591–596.

Kataoka M, Head JF, Persechini A, Kretsinger RH, Engelman DM. 1991. Small-angle X-ray scattering studies of calmodulin mutants with deletions in the linker region of the central helix indicate that the linker region retains a predominantly α-helical conformation. *Biochemistry 30*:1188–1192.

Kataoka M, Head JF, Seaton BA, Engelman DM. 1989. Melittin binding causes a large calcium-dependent conformational change in calmodulin. *Proc Natl Acad Sci USA 86*:6944–6948.

Kataoka M, Kuwajima K, Tokunaga F, Goto Y. 1997. Structural characterization of the molten globule of α-lactalbumin by solution X-ray scattering. *Protein Sci 6*:422–430.

Kataoka M, Nishii I, Fujisawa T, Ueki T, Tokunaga F, Goto T. 1995. Structural characterization of the molten globule and native states of apomyoglobin by solution X-ray scattering. *J Mol Biol 249*:215–228.

Khechinashvili NN, Privalov PL, Tiktopulo EL. 1973. Calorimetric investigation of lysozyme thermal denaturation. *FEBS Lett 30*:57–60.

Kippen AD, Sancho J, Fersht AR. 1994. Folding of barnase in parts. *Biochemistry 33*:3778–3786.

Konno T, Kamatari YO, Kataoka M, Akasaka K. 1997. Urea-induced denatured states of a protein, *Streptomyces* subtilisin inhibitor. *Protein Sci 6*:2242–2249.

Konno T, Kataoka M, Kamatari Y, Kanaori K, Nosaka A, Akasaka K. 1995. Solution X-ray scattering analysis of cold-, heat-, and urea-denatured states in a protein, *Streptomyces* subtilisin inhibitor. *J Mol Biol 251*:95–103.

Lattman EE. 1994. Small angle scattering studies of protein folding. *Curr Opin Struct Biol 4*:87–92.

Lehrman SR, Tuls JL, Lund M. 1990. Peptide α-helicity in aqueous trifluoroethanol: Correlations with predicted α-helicity and the secondary structure of the corresponding regions of bovine growth hormone. *Biochemistry 29*:5590–5596.

Loh SN, Kay MS, Baldwin RL. 1995. Structure and stability of a second molten globule intermediate in the apomyoglobin folding pathway. *Proc Natl Acad Sci USA 92*:5446–5450.

Nelson JW, Kallenbach NR. 1986. Stabilization of the ribonuclease S-peptide α-helix by trifluoroethanol. *Proteins Struct Funct Genet 1*:211–217.

Nelson JW, Kallenbach NR. 1989. Persistence of the α-helix stop signal in the S-peptide in trifluoroethanol. *Biochemistry 28*:5256–5261.

Nishii I, Kataoka M, Goto Y. 1995. Thermodynamic stability of the molten globule states of apomyoglobin. *J Mol Biol 250*:223–238.

Nishii I, Kataoka M, Tokunaga F, Goto Y. 1994. Cold denaturation of the molten globule states of apomyoglobin and a profile for protein folding. *Biochemistry 33*:4903–4909.

Ohgushi M, Wada A. 1983. "Molten-globule state": A compact form of globular proteins with mobile side chains. *FEBS Lett 164*:21–24.

Ptitsyn OB, Bychkova VE, Uversky VN. 1995. Kinetic and equilibrium folding intermediates. *Philos Trans R Soc Lond B 348*:35–41.

Saito S, Murao S. 1973. Isolation and crystallization of microbial alkaline protease inhibitor, S-SI. *Agric Biol Chem 37*:1067–1074.

Segawa S, Fukuno T, Fujiwara K, Noda Y. 1991. Local structure in unfolded lysozyme and correlation with secondary structures in the native conformation: Helix-forming or -breaking propensity of peptide segments. *Biopolymers 31*:497–509.

Shiraki K, Nishikawa K, Goto Y. 1995. Trifluoroethanol-induced stabilization of the α-helical structure of β-lactoglobulin: Implication for non-hierarchical protein folding. *J Mol Biol 245*:180–194.

Sosnick TR, Trewhella J. 1992. Denatured states of ribonuclease A have compact dimensions and residual secondary structure. *Biochemistry 31*:8329–8335.

Takano T. 1977a. Structure of myoglobin refined at 2.0 A resolution. I. Crystallographic refinement of metmyoglobin from sperm whale. *J Mol Biol 110*:537–568.

Takano T. 1977b. Structure of myoglobin refined at 2.0 A resolution. II. Structure of deoxymyoglobin from sperm whale. *J Mol Biol 110*:569–584.

Tanford C. 1970. Protein denaturation. C. Theoretical models for the mechanism of denaturation. *Adv Protein Chem 24*:1–95.

Ueki T, Hiragi Y, Kataoka M, Inoko Y, Amemiya Y, Izumi Y, Tagawa H, Muraga Y. 1985. Aggregation of bovine serum albumin upon cleavage of its disulfide bonds, studied by the time-resolved small-angle X-ray scattering technique with synchrotron radiation. *Biophys Chem 23*:115–124.

Uversky VN, Narizhneva NV, Kirschstein SO, Winter S, Lober GSO. 1997. Conformational transitions provoked by organic solvents in β-lactoglobulin: Can a molten globule like intermediate be induced by the decrease in dielectric constant? *Folding Design 2*:163–172.

van der Goot FG, Gonzales-Manes JM, Lakey JH, Pattus F. 1991. Molten globule membrane-insertion intermediate of the pore-forming domain of colicine-A. *Nature 354*:408–410.